INVESTIGATION OF NANO GRAPHENE COATING EFFECT ON MICRO-HARDNESS PROFILE AND MICROSTRUCTURE CHARACTERIZATION OF ST37 STEEL BY FRICTION-STIR-PROCESSING METHOD

[1]S. M. H. SHARIFI, [2]A. SABETGHADAM-ISFAHANI

[1]Associated Professor, Mechanical Engineering Department, Abadan Faculty, Petroleum University of Technology, Abadan, Iran
[2]Machinery Specialist, Persian Gulf Star Company, Bandar Abbas, Iran
E-mail: [1]Sharifi@put.ac.ir, [2]arminsabet1990@gmail.com

Abstract - In this research, 3 types of samples micro-hardness were investigated: 1. Friction Stir Processed (FSP) samples coated with Graphene Nano particles; 2. FSPed samples without any particle; 3. The Base Metal (BM). Then, the effect of applying FSP on St37 steel Micro-hardness with Graphene Nano-particles was investigated and then compared to the one of samples without any particle and the BM. In all FSPed samples, rotational and traverse speed were considered 900 rpm and 100 mm/min, respectively. All experiments were done in the same total dominant conditions. It is notable that Micro-hardness of three produced fabrication zones (Nugget Zone, TMAZ, HAZ) in both FSP Nano-coated sample and FSPed sample (without any particle) showed a great promotion in comparison to the one in BM. But, this promotion is not extended homogenous and equivalent in all three parts (Nugget Zone, TMAZ, HAZ) and in both two different samples (with and without Nano particles). Nugget zones experienced the biggest amount of promotion in Micro-hardness value in both FSP Nano-coated samples and FSPed samples. In addition, the FSPed Nano-coated samples allocated greater promotion slope to themselves. By comparing the three produced fabrication zones; it's concluded that coating Nano Graphene particles by FSP caused greater difference rather than the other samples.

Keywords - Friction Stir Processing, Graphene, St37 Steel, Micro-hardness.

I. INTRODUCTION

St37 steel has been widely used in the construction of pipelines in petroleum and gas industries. Micro-hardness is one of the key determinant factors in designing pipelines and weld metals. Recently, Micro-hardness has been extensively used in order to improve the mechanical properties of steels and weld metals. Mechanical property enhancements can be achieved using refinement of microstructures. Factors such as dispersion of active nucleation sites, austenite grain size, and cooling have great influence of formation of acicular ferrite [1-8]. Several types of ferrite structures may be encountered while studying the microstructure of weld metals; including grain boundary allotriomorphic ferrite, polygonal ferrite, Widmanstätten ferrite, and acicular ferrite. Allotriomorphic ferrite grows from columnar austenite grain boundaries and can sometimes be seen as almost continuous grain boundary layers with various thicknesses. Widmanstätten ferrite nucleates grow from the grain boundary allotriomorphic ferrite layers or austenite grain boundaries and develop into austenite grains in the form of thin wedge-shaped laths. Basically, there is a difference in nucleation between acicular ferrite and bainite that formed at the same temperature range and transformation mechanism. The fine interlocking microstructure of acicular ferrite nucleates intragranular in the form of separate laths from non-metallic inclusions within large austenite grains, whereas the bundle morphology of bainite grows at small austenite grains or austenite grain boundaries, forming sheaves of parallel laths [9, 10].

Weld metals show the best combination of strength and impact toughness in intergranular acicular ferrite, since density is increased in high-angled boundaries. Boundaries have different crystallographic orientation, therefore, they act like strong barriers and change crack growth direction [10-12]. In the two past few decades, the effectiveness of various non-metallic inclusions in producing intergranular ferrite in low alloy steels and weld metals has been investigated. Several factors, including the chemical composition, shape, size and distribution of inclusions, have strongly influenced the potential nucleation sites for the formation of intergranular ferrite [1, 2, 4-7, 13-19]. One of the newly introduced methods for microstructure refinement is a solid-state process called Friction Stir Processing (FSP) which uses the same approach as the Friction Stir Welding [20, 21]. A schematic view of FSP is depicted in Fig 1. In FSP, as a result of friction between the rotating tool and underlying substrate, the localized heating increases the local temperature of work piece to a range that plastic deformation can occur and fine grains are resulted [20]. Substrate plastic deformation and interaction between nanoparticles are limited due to the process temperature which is well below the melting point of the work piece. Thus, grain refinement and fabricating composite with FSP method is very attractive. Another approach of

microstructure refinement is Nano-coating with electrode, in which mechanical properties and microstructure of weld metals are enhanced by adding nanoparticles to conventional electrodes. For instance, adding nanoparticles such as TiO [6, 19], TiO2 [22, 23], and Ti2O3 [2, 13, 15] to low alloy steels and weld metals have positive effects on nucleating intragranular ferrite. Present investigation, compares the results from applying FSP method with CNT/ZrO2 nanoparticles on the improvement of Micro-hardness in Stir Zone (SZ), Heat Affected Zone (HAZ) and Thermo-Mechanic Affected Zone (TMAZ) with similar results from Nano-coating method in columnar zone and reheated zone [24]. Four different parts; BM, Nugget Zone, HAZ, and TMAZ is illustrated in Fig 2.

II. EXPERIMENTAL DETAILS

A. Chemical Composition

A 25.4 mm by 25.4 mm sample was sectioned from a corner of the plate using a Struers Sectom-10 diamond saw. This sample was sent for chemical analysis at Metallurgy Laboratory of Sharif Jahad, to determine the chemical composition of the steel used in this work. Table (1) gives the composition limits for St 37 steel according to MIL-S-16216K [19]. Chemical composition and mechanical properties of BM are presented in Table (1) and (2), respectively.

B. Micro-hardness

Herein, Vickers method (DPH) has been used for Micro-hardness evaluation. Test indenter was made of diamond and formed from right pyramid with a square base and an angle of 136 degrees. Samples were subjected to a load ranging between 1 to 100 KgF; the full load was applied for 10 to 15 seconds. Afterwards, when the load was removed, the two diagonals of the indentation left in the surface of the material were measured by a microscope and their average was calculated. Also, the area of the sloping surface of the indentation was calculated. The Vickers hardness was the quotient obtained by dividing the applied KgF load on the square millimeters area of the indentation, Eq. (1).

$$Micro - hardness \equiv Force\,(KgF)\,/\,A(mm^2) \quad (1)$$

C. Material Phase (Austenite, Ferrite, Pearlite)

A comparison between material phases shows that in austenite phase, grain boundaries can be recognized and the grain size is finer. In Ferrite phase, grain size is finer and more regular than pearlite phase; grain boundaries, however, are not as recognizable as in austenite phase. Pearlite phase, has structural turbidity and grain boundaries are not recognizable too. So as it is clear, having a region in austenite phase is much better than other phases; since, the grain sizes are more recognizable, grains are more regular, and the form of grains is more homogeneous.

St 37	Fe	C	Si	Mn	P
Magnitude	Base	0.131	0.0657	0.445	0.0092
St 37	S	Cr	Ni	Mo	Al
Magnitude	0.0207	0.0278	0.0286	0.0023	0.0403
St 37	Co	Cu	Nb	Ti	V
Magnitude	0.0045	0.0616	0.00072	0.00046	0.0023
St 37	W	Pb	Sn	As	Zr
Magnitude	0.0049	0.0023	0.0043	0.0029	0.00054

Table 1 Chemical Composition of St37 Steel.

	Nano Particle	E (GPa)	YTS (MPa)	Elongation (%)	YTS Promotion (%)
FSPed Sample	Graphene	196	392	2.5	86.6
Base Metal	-----	105	210	2.5	0.00

Table 2 Tensile Results for the FSPed Specimens in 1 Pass.

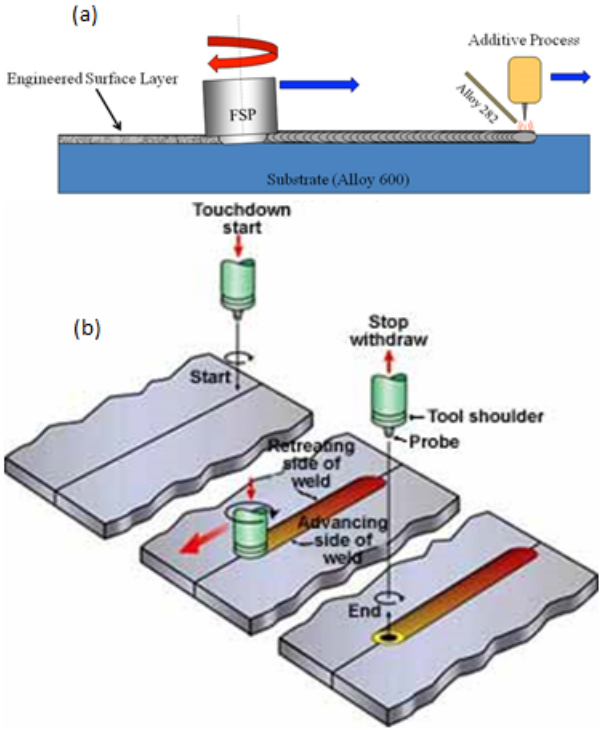


Figure 1 FSP Nomenclature; (a) Front View, (b) 3D View [4].

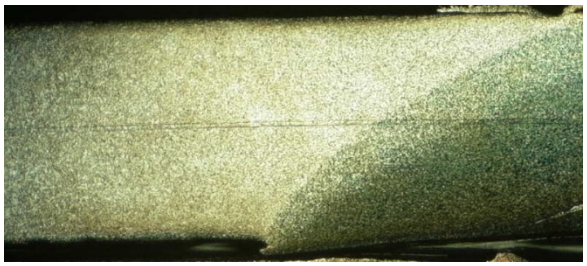


Figure 2 The conversion of the base metal into austenite phase in four steps; 1) BM, 2) HAZ, 3) TMAZ, 4) SZ.

All used Base Metals (BM) in these experiments were in Ferrite or Pearlite phases that is a negative point for samples and changing their phases by a process to austenite is a great benefit for the process. Concluded from the results that the chief advantage of the FSP method is gradually converting the BM's phase from pearlite or ferrite to austenite in four steps as shown in Fig.2.

D. Zones in FSP Nano-coating Method

There are three main produced zones in the work piece after applying the FSP method on it; these zones are named Stir Zone (SZ), Heat Affected Zone (HAZ), and Thermal and Mechanical Affected Zone (TMAZ). As it is clear from the zones' names, SZ is a region where the maximum value of the Nano particle is dispersed in it, and totally, the whole characteristics of the BM are changed both from point of mechanical and thermal view. These characteristics changes are perceptible in Micro and Macro scale. The second zone TMAZ, is a region where Nano particle is dispersed in it but not as much as SZ. In this region, the driving force of dispersion is combined from mechanical forces (caused by the pin traverse and rotational motion) and the thermal affects (caused by the friction). The third zone HAZ, is a region where its Nano particle is a little bit less than the TMAZ. In this region, the driving force of dispersion is only caused from the thermal affects. The Stir Zone (SZ) is the most noteworthy zone in the work piece, because unlike other two segments, Nano dispersion occurs mainly at this zone. Nano dispersion in all three mentioned zones are shown in Fig.2.

E. Procedure

Herein, the total procedure of the experiments is described which all had been done at room temperature. The BM used in this research was St37 steel of which chemical compositions and mechanical properties are listed in Table 1 and Table 2 respectively.

First, in FSP method seven work pieces were provided with lengths, widths, and thicknesses of 200, 150 and 2 mm respectively. A groove was then made by wire cut in a straight line along middle length of the three work pieces. Afterward, Graphene Nanoparticles with Aston were inserted into the grooves; and finally, FSP process with tool tilt angle of 3 degrees was done on the six prepared samples of work pieces (3 samples for FSPed Graphene coated, and 3 for just FSPed samples), and One was kept as the BM. The rotational and traverse speed were 900 rpm and 100 mm/min, respectively.

Second, a piece of FSPed samples (with and without Nano particle) including; BM, HAZ, TMAZ, and SZ were cut to undergo DPH test. The mechanism of the DPH is choosing 3 points from each region (BM, HAZ ...) and obtaining the average value of the hardness there. Then combining these obtained average values as a profile which is called Micro-hardness profile.

III. RESULTS AND DISCUSSION (MICRO-HARDNESS TEST RESULTS)

Herein, the obtained Micro-hardness results of two different kinds of samples, one FSPed with Graphen Nano particles and the other FSPed without any particle, have been shown in Fig.3 and Fig.4, respectively, simultaneously compared with the BM; and eventually are compared with each other in Table 3.

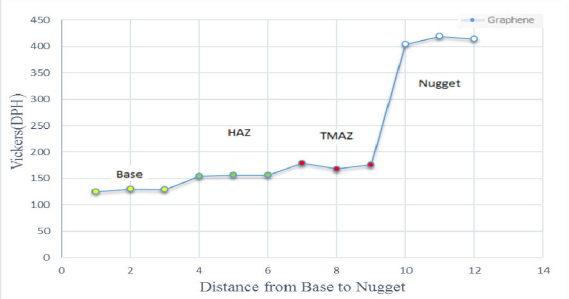


Figure 3 Micro-hardness profile in four different parts for FSPed sample with Nano Graphene particles.

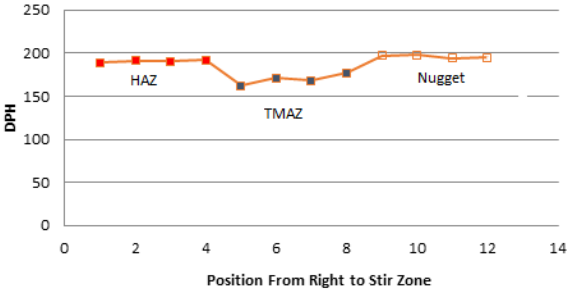


Figure 4: Micro-hardness profile in three different parts for FSPed sample without any particle.

Nano Particle			Micro-hardness			
			BM	HAZ	TMAZ	SZ
Samples	FSPed	Without any Particle	128	176	158	198
	FSPed	Graphene	128	155	174	412

Table 3 Comparison of Obtained Micro-hardness Results from Two Different Nano particles.

This promotion of Micro-hardness in FSP, is caused by the process in which the microstructure of the work piece changes from perlite (In BM) to austenite (In SZ). This change in microstructure results caused from Zener Pinning Effect (ZPE) which states that by decreasing the grain size of the particles, more energy is stored on the grain boundaries which produces more regular grains and smaller grain sizes. The bases of ZPE is measuring the effect of fine particles dispersion on the movement of low-and high angle grain boundaries through a polycrystalline material. Small particles act to prevent the motion of such boundaries by exerting a pinning pressure which counteracts the driving force pushing the boundaries. The

mathematical description of the ZPE is so important. The Fig. 5 illustrates a boundary of energy γ per unit area where it intersects with an incoherent particle of radius r. The pinning force acts along the line of contact between the boundary and the particle i.e. a circle of diameter AB=2πrcosθ. The force per unit length of boundary in contact is γsinθ. Hence, the total force acting on the particle-boundary interface is:

$$F = 2\pi r\gamma \cos\theta \sin\theta \quad (2)$$

The maximum restraining force occurs when:

$$\theta = 45° \quad \text{and so} \quad F_{\max} = \pi r\gamma \quad (3)$$

In order to determine the pinning force by a given dispersion of particles, Clarence Zener made several important assumptions [25]:

- The particles are spherical.
- The passage of the boundary does not alter the particle-boundary interaction.
- Each particle exerts the maximum pinning force on the boundary regardless of contact position.
- The contacts between particles and boundaries are completely random.
- The number density of particles on the boundary is that expected for a random distribution of particles.

For a volume fraction F_v of randomly distributed spherical particles of radius r, the number per unit volume (number density) is given by:

$$N_{Total} = (3F_v)/(4\pi r^3) \quad (4)$$

Given the assumption that all particles apply the maximum pinning force, F_{max} the total pinning pressure exerted by the particle distribution per unit area of the boundary is:

$$P_s = N_{Interact} F_{\max} = (3F_v\gamma)/(2r) \quad (5)$$

Only particles within one radius (solid circles) can intersect a planar boundary, Fig.6. This is referred to as the Zener pinning pressure. It follows that large pinning pressures are produced by:

- Increasing the volume fraction of particles.
- Reducing the particle size.

The Zener pinning pressure is orientation dependent, which means that the exact pinning pressure depends on the amount of coherence at the grain boundaries [25].

According to the formula (1) and (2), the more spherical and homogenous grains, the more force on the grains' boundaries, and the more force on the grains' boundaries the more benefited composite. As it is clear from formula (3) and (4), the real magnitude of P_s cannot be calculated, but approximately can be observed. These approximate results are presented in Table 4. According to the results of Table 4, it can be concluded that the pressure on the Graphene coated steel borders is more than the FSPed sample without any particle; so it produces smaller grains. Herein, the more benefited composite refers to promoting a metal from characteristics point of view by an efficient technique and using optimized level of special Nano-particles. In this research this benefited composite has been produced by FSP technique and optimized level of Graphene Nano particles.

The microstructure of BM and SZ of FSPed sample without any particle are shown in Fig.7. As it is observed, in FSP the greatest amount of Micro-hardness belongs to SZ and then reduces gradually by passing from HAZ to TMAZ and BM, respectively.

It is noteworthy to mention that in FSPed Graphene Nano-coating method, there is more promotion in the microstructure of the work piece, Fig.8. This happens because of more homogeneous distribution of Nano Graphene particles, and consequently, having more boundary energy and more homogeneous grain sizes. According to ZPE, having less homogeneous grain sizes shows less grain boundaries' energy. Therefore, there is more irregularity in grain sizes which prevents microstructure changings, namely just FSPed sample in comparison to FSPed Nano Graphene coated sample.

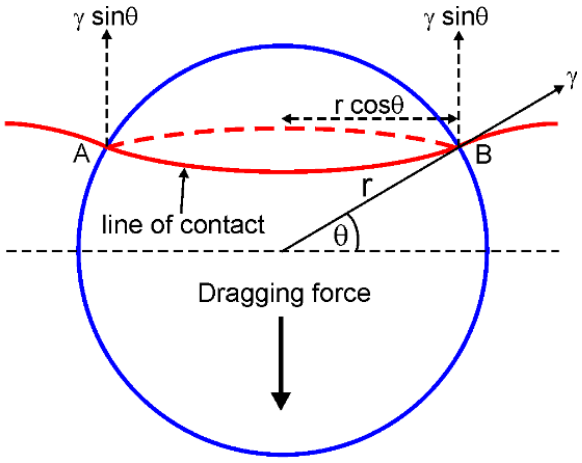


Figure 5 Schematic of the interaction a boundary and a particle.

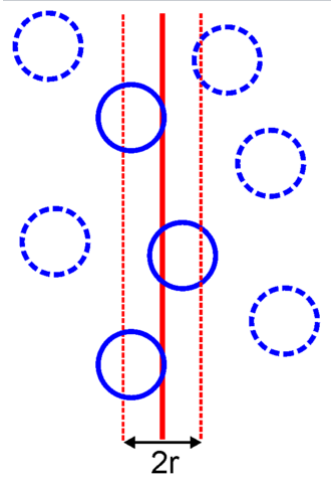


Figure 6 Only particles within one radius (solid circles) can intersect a planar boundary [25].

IV. CONCLUSION

St37 BM hardness value was reported 128 on the diamond pyramid hardness scale (DPH). The variance between BM and other three zones (SZ, HAZ, and TMAZ) is due to the non-homogenous nature of the material, including porosity and inclusion stringers. The results form martensitic microstructures produced by FSP show by approaching the TMAZ in the dry FSP microstructure, there is a gradual increase in hardness that peaks; it must be mentioned that the rate at which the hardness increases is at its greatest value in HAZ for just FSPed sample and in SZ for FSPed with Nano Graphene sample, but the maximum hardness value occurs in SZ. For instance, the increase of hardness for just FSPed sample from BM to HAZ is much more than its changes in TMAZ to SZ; but, for Graphene, the hardness changes from TMAZ to SZ is in its maximum magnitude, and totally, the highest value of Micro-hardness is for SZ of Graphene.

The hardness reaches its maximum and stays constant across the stir nugget –which also refers to SZ. Upon reaching the TMAZ, the hardness gradually decreases until the microstructure reaches the BM, Fig.3-4. This is attributed to its greater hardness value achieved by uniform dispersion of Nano Graphene reinforcements and using FSP. Extra contribution goes to severe plastic deformation that promoted grain refinement by dynamic recrystallization process. As it is clear, the promotion magnitude occurred for FSP. But the increase in Nano Graphene FSP coating is significantly greater than the growth in FSPed samples without any particle. The differences between just FSPed sample and Nano Graphene FSPes samples are:

- First, in Graphene FSP coating, SZ has martensitic microstructure and more homogeneous grain sizes.
- Second, from the figures, it can be observed that in FSP method, Micro-hardness values have minor differences in SZ and TMAZ for just FSPed sample but not for Graphene. In FSP Nano-coating method, however, there is drastically changes in hardness values as we move toward the reheated zone.

Overall, it can be concluded that FSP is an efficient method to promote metal hardness.

ACKNOWLEDGEMENT

The authors would like to acknowledge Persian Gulf Star Oil Company (P.G.S.O.C.) and Mr. M. A. Dadvar (the chief executive officer of P.G.S.O.C.), for financial and spiritual supports and also preparing a suitable atmosphere for promotion of skilled and talented employees.

REFERENCES

[1] W. W. Bose-Filho, A. L. M. Carvalho, and M. Strangwood, "Effects of alloying elements on the microstructure and inclusion formation in HSLA multipass welds," Materials characterization, Vol. 58(1), pp. 29-39, (2007).
[2] J. S. Byun, et al., "Inoculated acicular ferrite microstructure and mechanical properties," Materials Science and Engineering: A, Vol. 319, pp. 326-331, (2001).
[3] M. Calcagnotto, D. Ponge, and D. Raabe, "Effect of grain refinement to 1μm on strength and toughness of dual-phase steels," Materials Science and Engineering: A, Vol. 527(29), pp. 7832-7840, (2010).
[4] S.A. Court, and G. Pollard, "Inclusion chemistry and morphology in shielded metal arc (SMA) steel weld deposits", Metallography, Vol. 22(3), pp. 219-243, (1989).
[5] T. Pan, Z.-G Yang, C. Zhang, B.-Z. Bai, H.-S. Fang, "Kinetics and mechanisms of intragranular ferrite nucleation on non-metallic inclusions in low carbon steels," Materials Science and Engineering: A, Vol. 438, pp. 1128-1132, (2006).
[6] S. St-Laurent, and G. L'Espérance, "Effects of chemistry, density and size distribution of inclusions on the nucleation of acicular ferrite of Mn steel shielded-metal-arc-welding weldments," Materials Science and Engineering: A, Vol. 149(2), pp. 203-216, (1992).
[7] S. Terashima, S.z and H. Bhadeshia, "Size distribution of oxides and toughness of steel weld metals", Science and Technology of Welding and Joining, Vol. 11(5), pp. 580-582, (2006).
[8] C. Wang, et al., "Effect of microstructural refinement on the toughness of low carbon martensitic steel," Scripta Materialia, Vol. 58(6), pp. 492-495, (2008).
[9] S.S. Babu, "The mechanism of acicular ferrite in weld deposits," Current opinion in Solid state and Materials Science, Vol. 8(3), pp. 267-278, (2004).
[10] H. Bhadeshia, "Bainite in steels: transformation, microstructure and properties," IOM Communications, London, Vol. 42, pp. 237-276, (2001).
[11] M. Diaz-Fuentes, A. Iza-Mendia, and I. Gutierrez, "Analysis of different acicular ferrite microstructures in low-carbon steels by electron backscattered diffraction. Study of their toughness behavior," Metallurgical and Materials Transactions A, Vol. 34(11), pp. 2505-2516, (2003).
[12] H. Flower, and T. Lindley, "Electron backscattering diffraction study of acicular ferrite, bainite, and martensite steel microstructures," Materials Science and Technology, Vol. 16(1), pp. 26-40, (2000).
[13] J.-S. Byun, J.-H. Shim, and Y.W. Cho, "Influence of Mn on microstructural evolution in Ti-killed C–Mn steel," Scripta Materialia, Vol. 48(4), pp. 449-454, (2003).
[14] M.D. Fuentes, I.M., I. Gutiérrez, "Energy Absorption", Materials Science Forum, Vol, 32, pp. 245–252, (1998).
[15] Y.Peng, W. Chen, and Z. Xu, "Study of high toughness ferrite wire for submerged arc welding of pipeline stee,l" Materials characterization, Vol. 47(1), pp. 67-73, (2001).
[16] J.-H. Shim, et al., "Nucleation of intragranular ferrite at Ti2O3 particle in low carbon steel," Acta Materialia, Vol. 47(9), pp. 2751-2760, (1999).
[17] J.-H. Shim, et al., "Ferrite nucleation potency of non-metallic inclusions in medium carbon steels," Acta Materialia, Vol. 49(12), pp. 2115-2122, (2001).
[18] K. Wu, "Three-dimensional analysis of acicular ferrite in a low-carbon steel containing titanium," Scripta materialia, Vol. 54(4), pp. 569-574, (2006).
[19] D. Zhang, H. Terasaki, and Y.-i. Komizo, "In situ observation of the formation of intragranular acicular ferrite at non-metallic inclusions in C–Mn steel," Acta materialia, Vol. 58(4), pp. 1369-1378, (2010).
[20] Z. Ma, "Friction stir processing technology: a review," Metallurgical and Materials Transactions A, Vol. 39(3), pp. 642-658, (2008).

[21] R.S. Mishra, and Z. Ma, "Friction stir welding and processing", Materials Science and Engineering: R: Reports, Vol. 50(1), pp. 1-78, (2005).
[22] M. Kiviö, L. Holappa, and T. Iung, "Addition of dispersoid titanium oxide inclusions in steel and their influence on grain refinement," Metallurgical and Materials Transactions B, Vol. 41(6), pp. 1194-1204, (2010).
[23] S.H. Nedjad, and A. Farzaneh, "Formation of fine intragranular ferrite in cast plain carbon steel inoculated by titanium oxide nanopowder," Scripta Materialia, Vol. 57(10), pp. 937-940, (2007).
[24] M. Fattahi, et al., "Improvement of impact toughness of AWS E6010 weld metal by adding TiO2 nanoparticles to the electrode coating," Materials Science and Engineering: A, Vol. 528(27), pp. 8031-8039, (2011).
[25] C. C. Koch, R.O. Scattergood, K.A. Darling, and J.E. Semones, "Mechanical Properties," Journal of Materials Science: Vol. 43, pp. 7261-7264, (2008).

★★★